Supporting information for

Real-world identification of high-emitting vehicles based on near-road sensor measurement

Bo Li[1], Dongbin Wang (✉)[1], Qiang Zhang[1], Leqi Shi[1], Mingliang Fu[2], Hang Yin[2], Jingkun Jiang (✉)[1]

1 State Key Joint Laboratory of Environment Simulation and Pollution Control, School of Environment, Tsinghua University, Beijing 100084, China

2 Vehicle Emission Control Center, Chinese Research Academy of Environmental Sciences, Beijing 100012, China

✉ Corresponding authors

E-mail: wdb2016@tsinghua.edu.cn (D. Wang); jiangjk@tsinghua.edu.cn (J. Jiang)

One Text and 9 Figures

Text S1 Design of the newly developed CPC

Fig. S1 Comparison of the newly developed CPC (tested CPC) and TSI 3722 CPC.

Fig. S2 The percentage distribution of vehicle types (a, d), histograms of vehicle speeds (b, e), and wind rose plots (c, f) with wind speed in m/s recorded at Tangshan and Chengdu sites over the measurement period.

Fig. S3 The workflow scheme of high-emitting vehicle identification via HEI measurement.

Fig. S4 The impacts of time windows and lowest percentile values on the roadside measurement emission factor calculated of NO. (a) 1 min time window and lowest 10 values mean, (b) 5 min time window and lowest 1 percentiles, (c) 5 min time window and lowest 5 percentiles, (d) 5 min time window and lowest 10 percentiles, (e) 5 min time window and lowest 20 percentiles, (f) 5 min time window and lowest 30 percentiles.

Fig. S5 The pollutant concentration peak appeared times and time different of PN, NO, and CO_2 after the vehicles drove past the HEI platform. (a) peak appeared times of PN, NO, and CO_2, (b) time different between PN, NO and CO_2.

Fig. S6 The measured concentration, background concentration, and identified vehicles and corresponding emission factors at Chengdu from 8:05 a.m. to 8:30 a.m. of 6 May 2023.

Fig. S7 The percentages of HEI and RS identified and unidentified vehicles at (a) Tangshan and (b) Chengdu sites.

Fig. S8 Individual vehicle EF_{NO} (a) and EF_{PN} (b) for different vehicle and fuel types at Tangshan and Chengdu summary. Box plots show the Q1-1.5IQR and Q3 + 1.5IQR (lower and upper extent of whiskers, respectively), first and third quartile (bottom and top edge of the box, respectively), and median (centerline of the box). Circular dots are the points > Q3 + 1.5IQR.

Fig. S9 The percentages of HEI identified high-emitters at Tangshan and Chengdu sites for (a) including fleets and (b) excluding fleets.

1 Text

Text S1 Design of the newly developed CPC

In this study, a low-cost and compact CPC was developed for particle number (PN) measurement. Detailed information of the design and performance evaluation of this CPC can be found in previous study (Li et al., 2024). In brief, this CPC utilizes a laminar-flow structure with three major components of saturator, condenser, and adjustable optical detector. The working fluid used for the developed CPC is alcohol. The aerosol particles flow to the saturator with a flow rate of 0.3 LPM, then together with saturator working fluid vapors go downstream to the consider where particles grow. Finally, the grown particles are detected optically when passing through the waist of the laser beam. The overall cost of this CPC is generally below 1000 USD. Before usage, laboratory experiment is conducted to calibrate the CPC counting efficiency. Where, the saturator and condenser temperature are set as 39℃ and 17.5℃, respectively, the CPC bottom cut off particle size is measured to be 10 nm. In addition, the performance of the developed CPC was evaluated by comparing it with the CPC TSI-3772 (USA). As shown in Fig. S1, there is a good agreement between the developed CPC and the CPC TSI-3772 with the slope and R^2 values of 1.03 and 0.999, respectively.

Nine Figures

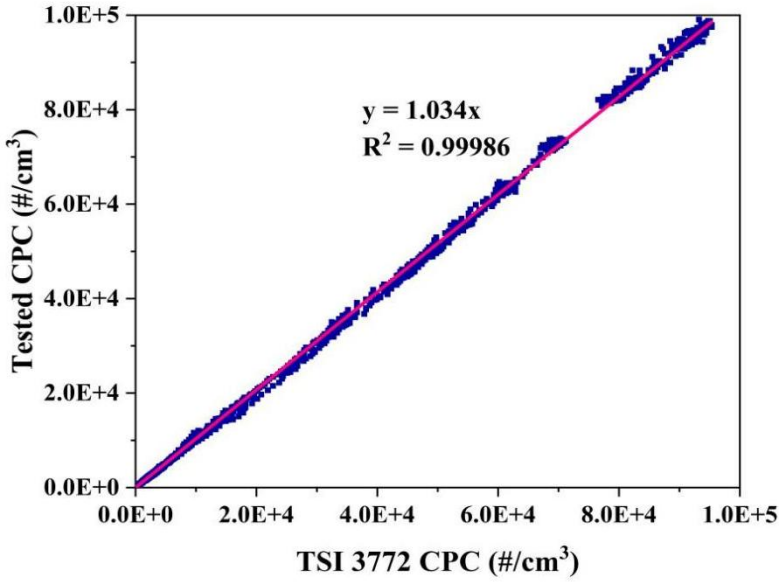

Fig. S1 Comparison of the newly developed CPC (tested CPC) and TSI 3722 CPC.

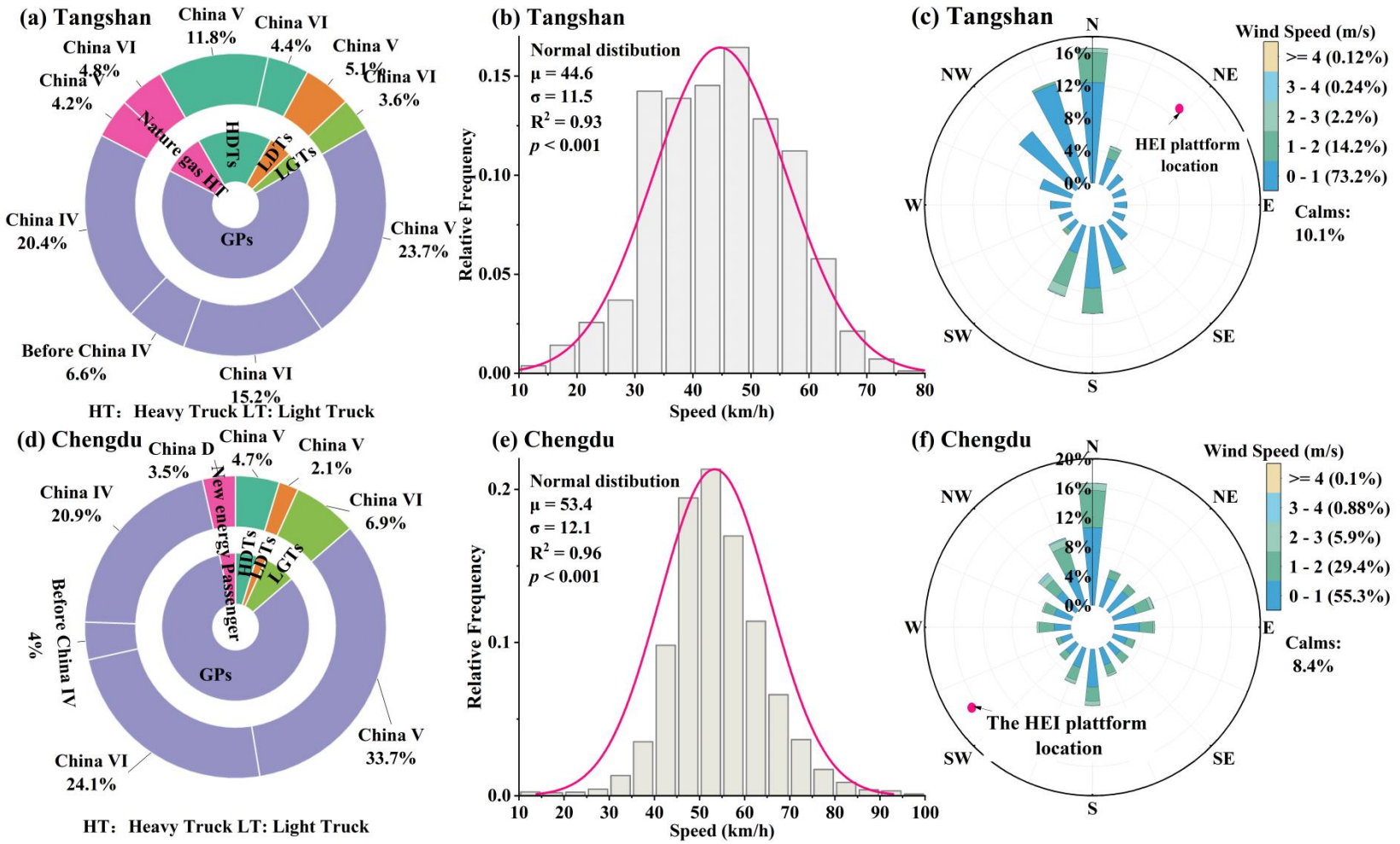

Fig. S2 The percentage distribution of vehicle types (a, d), histograms of vehicle speeds (b, e), and wind rose plots (c, f) with wind speed in m/s recorded at Tangshan and Chengdu sites over the measurement period.

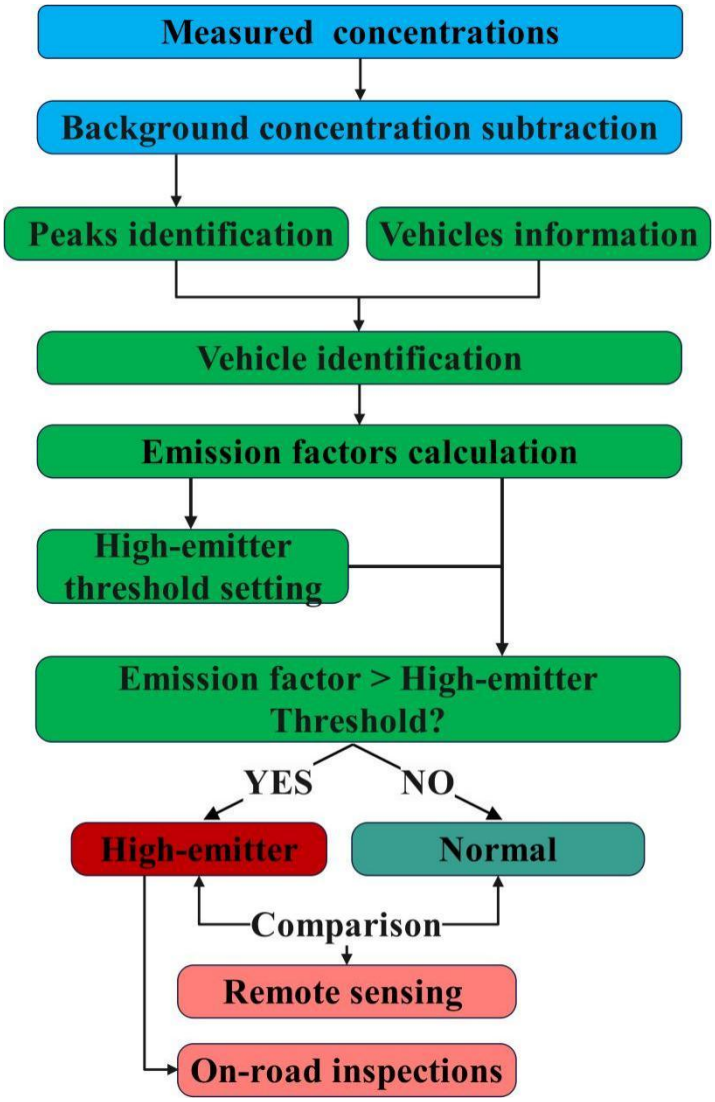

Fig. S3 The workflow scheme of high-emitting vehicle identification via HEI measurement.

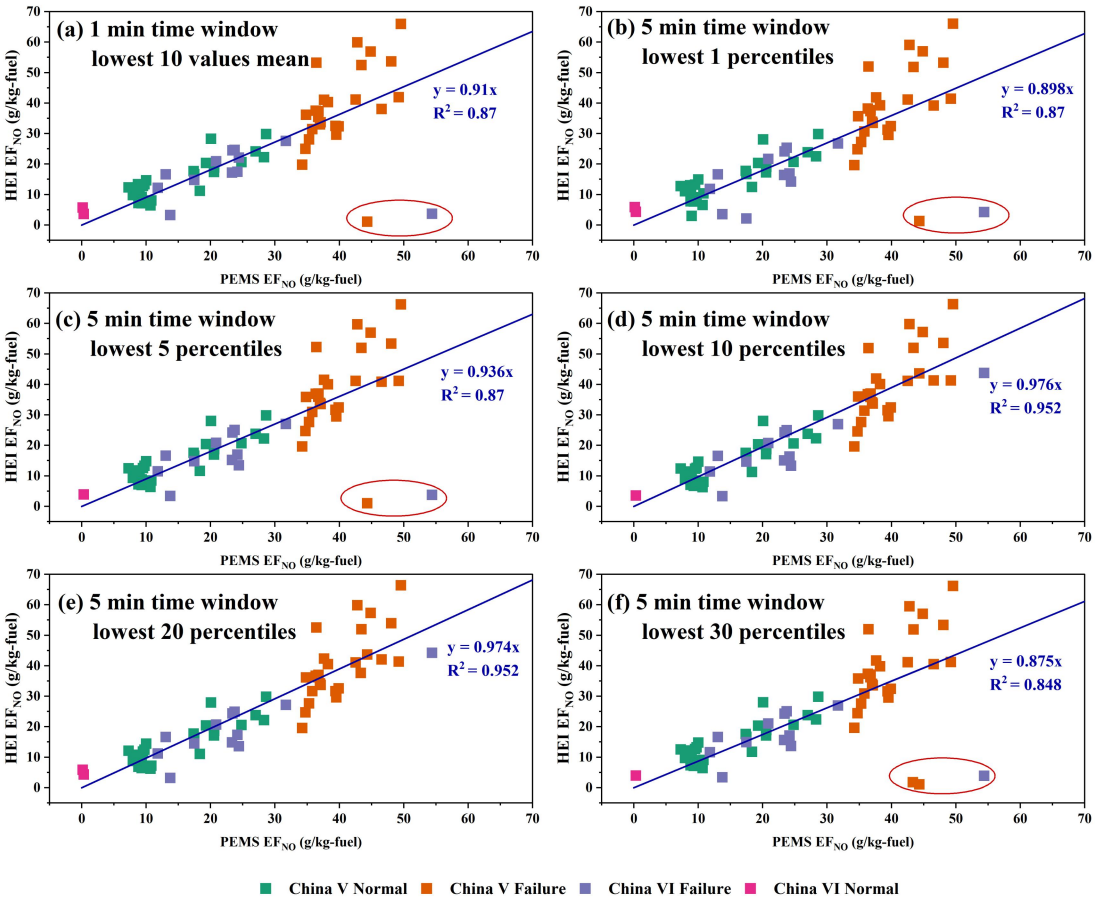

Fig. S4 The impacts of time windows and lowest percentile values on the roadside measurement emission factor calculated of NO. (a) 1 min time window and lowest 10 values mean, (b) 5 min time window and lowest 1 percentiles, (c) 5 min time window and lowest 5 percentiles, (d) 5 min time window and lowest 10 percentiles, (e) 5 min time window and lowest 20 percentiles, (f) 5 min time window and lowest 30 percentiles.

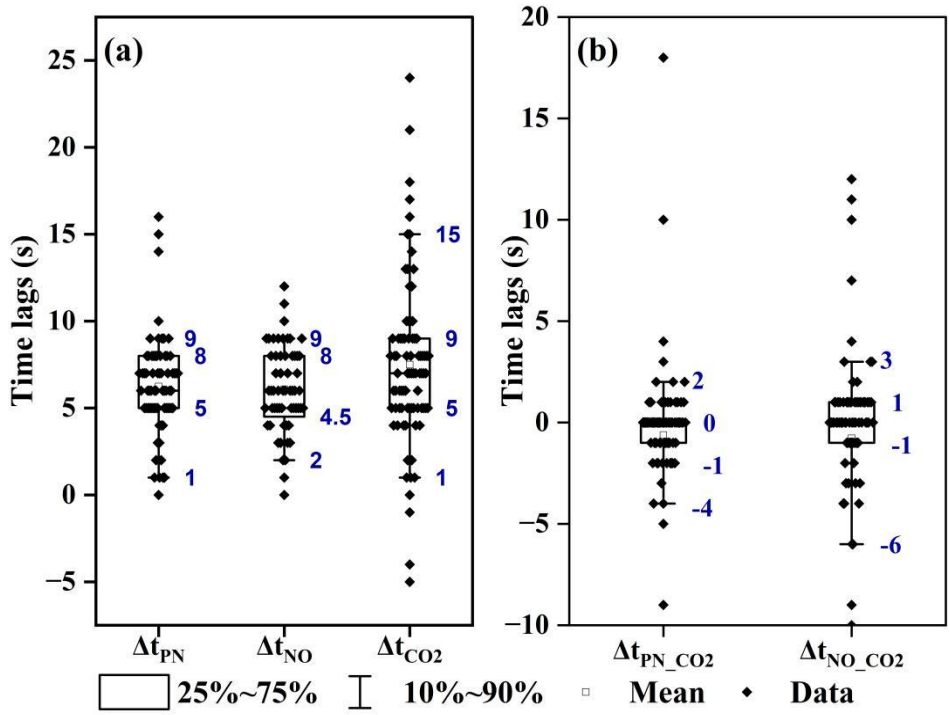

Fig. S5 The pollutant concentration peak appeared times and time different of PN, NO, and CO_2 after the vehicles drove past the HEI platform. (a) peak appeared times of PN, NO, and CO_2, (b) time different between PN, NO and CO_2.

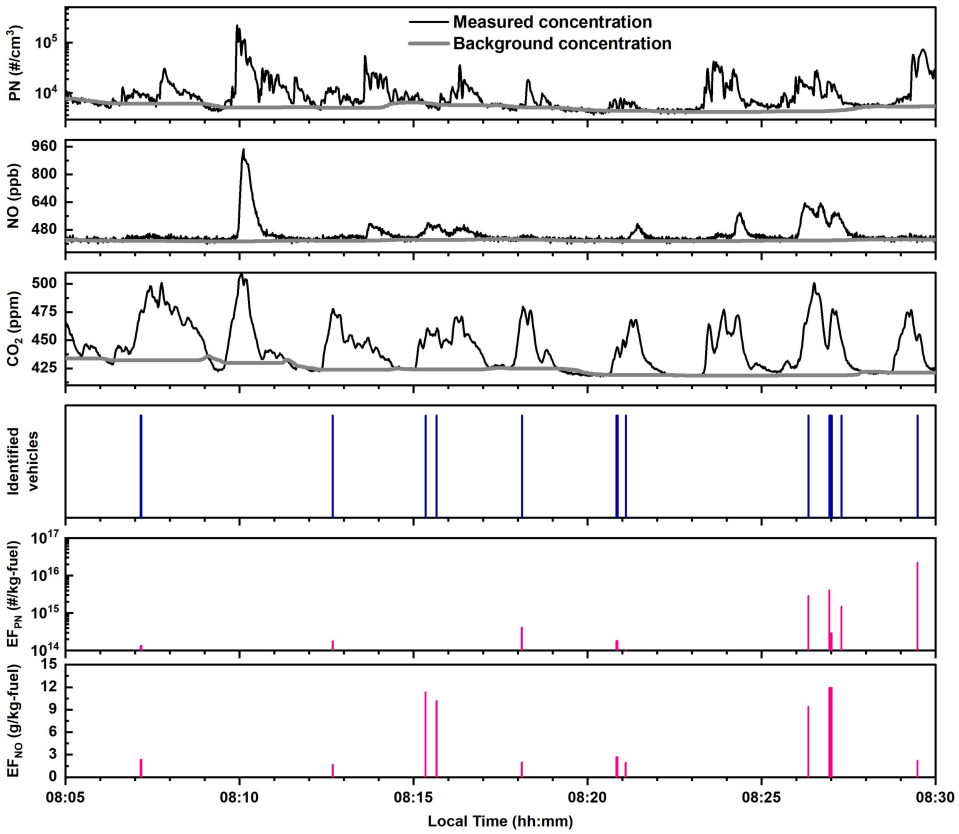

Fig. S6 The measured concentration, background concentration, and identified vehicles and corresponding emission factors at Chengdu from 8:05 a.m. to 8:30 a.m. of 6 May 2023.

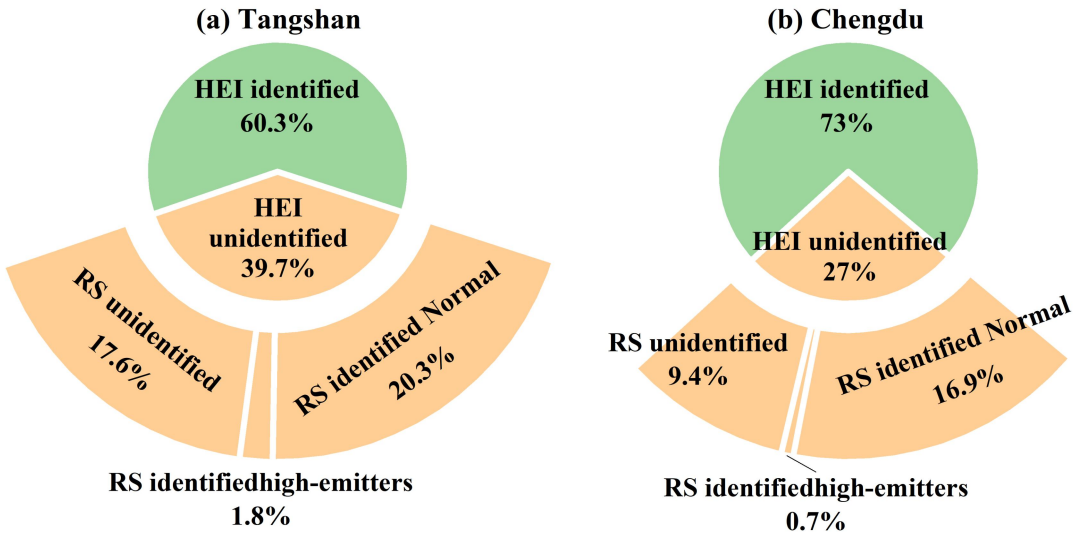

The percentages of HEI identified and unidentified vehicles at (a) Tangshan and (b) Chengdu

Fig. S7 The percentages of HEI and RS identified and unidentified vehicles at (a) Tangshan and (b) Chengdu sites.

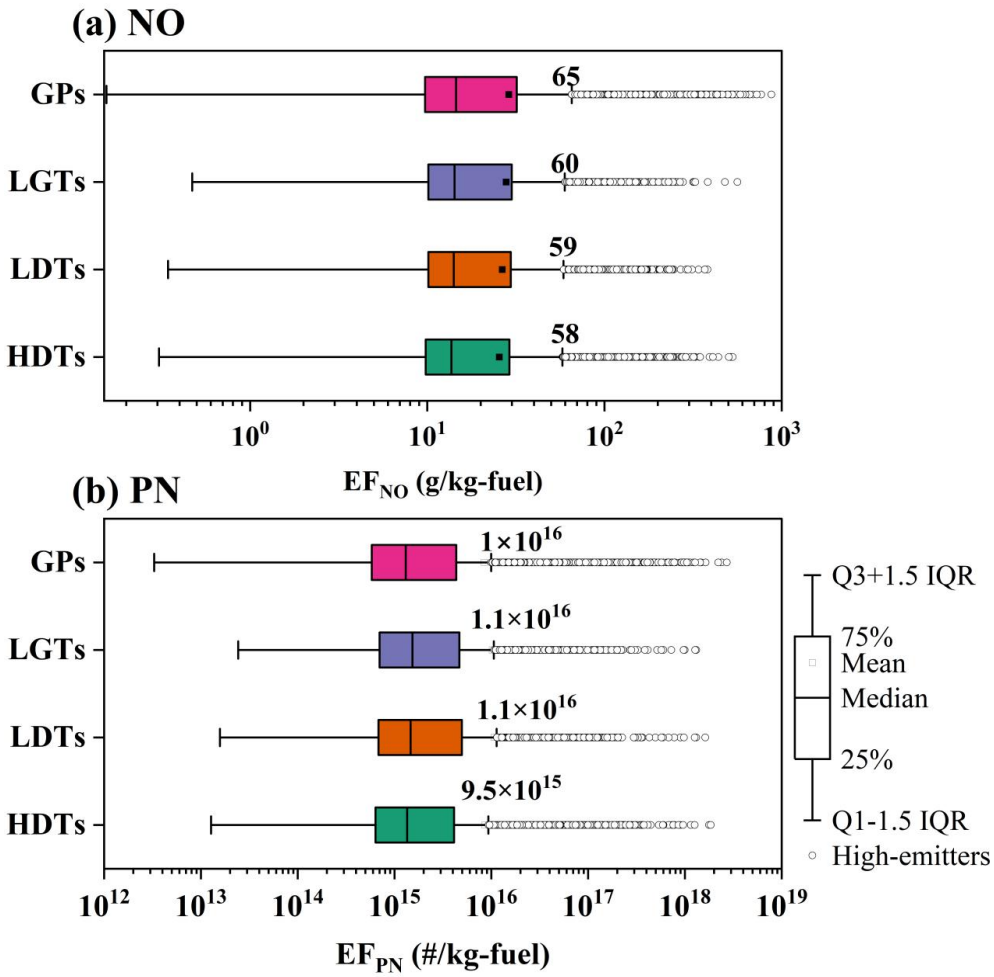

Fig. S8 Individual vehicle EF_{NO} (a) and EF_{PN} (b) for different vehicle and fuel types at Tangshan and Chengdu summary. Box plots show the Q1-1.5IQR and Q3 + 1.5IQR (lower and upper extent of whiskers, respectively), first and third quartile (bottom and top edge of the box, respectively), and median (centerline of the box). Circular dots are the points > Q3 + 1.5IQR.

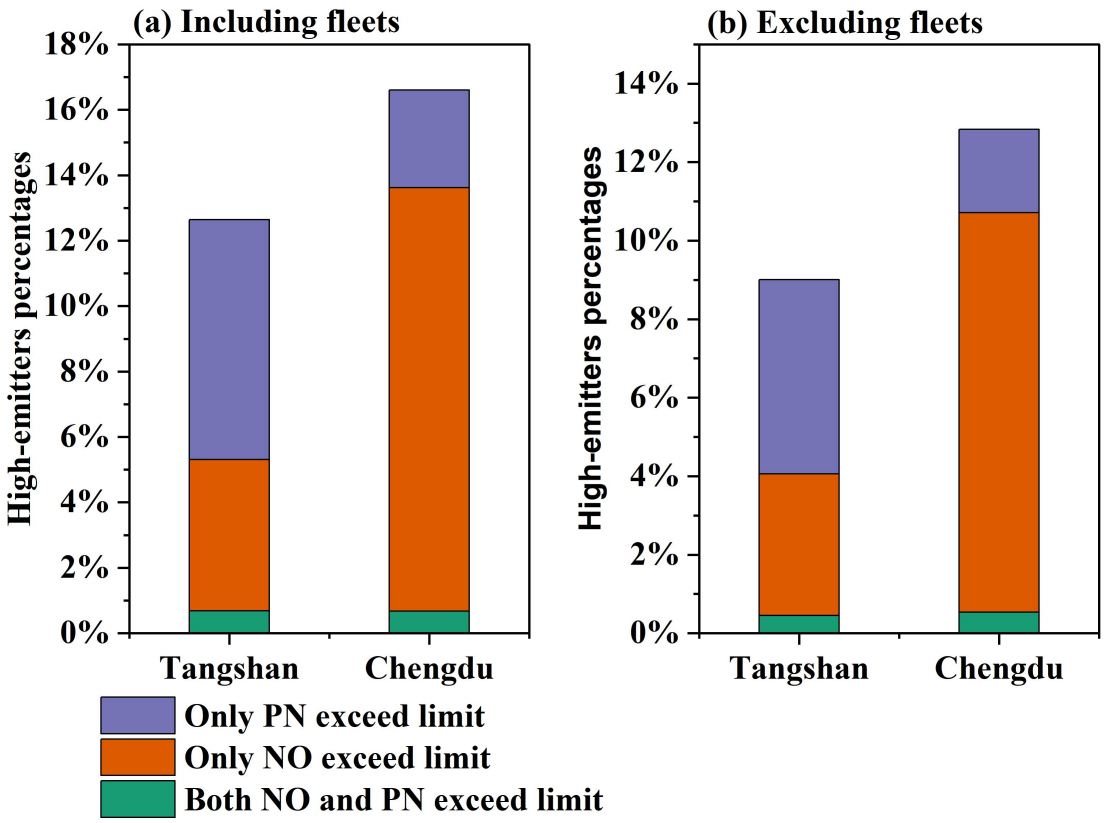

Fig. S9 The percentages of HEI identified high-emitters at Tangshan and Chengdu sites for (a) including fleet and (b) excluding fleet.

References

Li Y, Chen X, Wu J, Zhang Q, Zhang Z, Hao J, Jiang J (2024). A convertible condensation particle counter using alcohol or water as the working fluid. Aerosol Science and Technology, 59(2): 185–194 doi:10.1080/02786826.2024.2395939